ACS OMEGA

http://pubs.acs.org/journal/acsodf

Article

Identify Functional lncRNAs in Nonalcoholic Fatty Liver Disease by Constructing a ceRNA Network

Wei Xue, Jia Zhang, Yali Zhu, and Wenxiang Huang*

Cite This: *ACS Omega* 2022, 7, 22522−22530

Read Online

ACCESS | Metrics & More | Article Recommendations | Supporting Information

ABSTRACT: *Aim*: To identify functional long noncoding RNAs (lncRNAs) by constructing a NAFLD-related lncRNA−miRNA−mRNA network (NLMMN) based on the hypothesis that lncRNAs, as competitive endogenous RNAs (ceRNAs), are able to regulate mRNA functions by competitive binding to shared miRNAs. *Methods*: The "Limma R package" was used to identify differentially expressed lncRNAs and mRNAs (DElncRNAs and DEmRNAs). The "miRcode online tool" was used to predict the potential interactions between DElncRNAs or DEmRNAs using Perl, and "multiMiR R package" was used to predict the potential interactions between DElncRNAs and miRNAs. The NLMMN was viewed by Cytoscape. The DEmRNAs were further analyzed by Gene Ontology (GO) and Kyoto Encyclopedia of Genes and Genomes (KEGG) enrichment analysis. The real-time quantitative reverse transcription polymerase chain reaction (qRT−PCR) was used to identify functional lncRNAs in human liver tissue and FFAs-induced fat-overloading HepG2 cells. The role of functional lncRNA was explored in the HepG2 cell line. *Results*: A total of 336 DElncRNAs (154 upregulated and 182 downregulated, |log 2 (fold change)| >0.655 and $P < 0.05$) and 399 DEmRNAs (152 upregulated and 247 downregulated, |log 2 (fold change)| >0.608 and $P < 0.05$) were identified. A total of 142 DElncRNA-miRNA interaction pairs and 643 miRNA−DEmRNA interaction pairs were retained to construct the NLMMN, which contained 19 lncRNAs, 47 miRNAs, and 228 mRNAs. The results of GO and KEGG enrichment analyses were related to an extracellular matrix (ECM). Two upregulated lncRNAs (LINC00240 and RBMS3-AS3) and one downregulated lncRNA (ALG9-IT1) were identified by qRT−PCR in liver tissues. But only LINC00240 was significantly upregulated in fat-overloading HepG2 cells. Overexpression of LINC00240 did not affect lipid accumulation but increased the reactive oxygen species (ROS) content in HepG2 cells. *Conclusion*: LINC00240, RBMS3-AS3, and ALG9-IT1 might be novel functional lncRNAs that attenuate liver fibrosis in NAFLD by influencing the ECM through the ceRNA network. Among them, LINC00240 might have a key role.

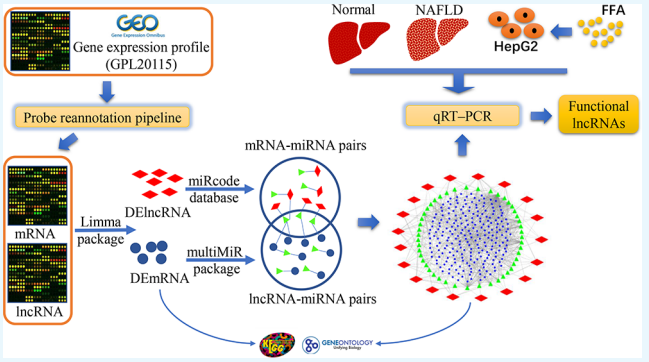

1. INTRODUCTION

Nonalcoholic fatty liver disease (NAFLD) does not refer to a certain disease but a spectrum of clinical and pathological severities, including simple steatosis, nonalcoholic steatohepatitis (NASH), fibrosis, cirrhosis, and even hepatocellular carcinoma (HCC).[1,2] The previous "second-hit hypothesis" proposed that the accumulation of lipids in the cytoplasm of liver cells (the first hit) triggers a series of cytotoxic events (the second hit) that lead to liver inflammation. The hypothesis has been updated to the "parallel multiple hits hypothesis",[3] which indicates that NAFLD should not be understood as a pathological "continuous spectrum" but a heterogeneous disease that takes different factors together to lead to liver inflammation and fibrosis by unknown pathways. In short, the pathogenesis of NAFLD is very complicated.[4] The current global prevalence of NAFLD is approximately 25.24%.[5] Over the past several decades, the prevalence of NAFLD has increased significantly worldwide.[2] A study showed that NASH is the most rapidly growing cause of HCC among patients who are listed for liver transplantation in the United States.[6] The clinical and economic burden of NAFLD has become enormous.[5,7] Therefore, we urgently need to explore emerging examination and treatment targets.

Over the years, protein-coding genes and their regulatory networks have been studied extensively. The development of transcriptomics and proteomics has revealed the regulatory role of noncoding RNAs (ncRNAs), a type of RNA that has no protein translation ability on gene expression and function.[8] Transcripts, mostly noncoding, cover 62−75% of our genome and contribute a lot to the overall estimate of 80% of the

Received: March 24, 2022
Accepted: June 9, 2022
Published: June 22, 2022

potential functional sequences in our DNA.[9] Long noncoding RNAs (lncRNAs), which are greater than 200 nucleotides in length, account for the majority of ncRNAs.[10,11] LncRNAs play important roles in the pathophysiology of many diseases.[11] An increasing number of studies have shown that lncRNAs are an emerging class of metabolic regulators.[12] Although many studies have explored the role of lncRNA in the development of NAFLD,[13] they remain largely unknown.

Recent studies have shown that lncRNAs, as competitive endogenous RNAs (ceRNAs) with microRNA (miRNA) response elements, can compete with mRNAs by competitive binding to shared miRNAs, thus affecting gene expression.[14] Considering the potential relevance of lncRNAs in the development of NAFLD through the ceRNA mechanism, in this study, we used bioinformatics tools to construct a NAFLD-related lncRNA−miRNA−mRNA network (NLMMN) to identify functional lncRNAs that might impact the development of NAFLD. The role of lncRNAs in NAFLD can be further explored by analyzing the NLMMN, which may bring new ideas for the diagnosis and treatment strategies of NAFLD. Consequently, it is necessary to investigate the role of the ceRNA network in NAFLD.

2. MATERIAL AND METHODS

2.1. Gene Expression Profile. LncRNA and mRNA expression profiles from the GSE107231 dataset were acquired from the Gene Expression Omnibus (GEO) database (https://www.ncbi.nlm.nih.gov/geo/). After acquiring the data, the Limma package in R 4.0.0 (the R Foundation for Statistical Computing, Vienna, Austria) was used to normalize the gene expression of each sample.

2.2. Probe Reannotation Pipeline. The probe sequences of the GPL20115 platform were downloaded from the GEO database (https://ftp.ncbi.nlm.nih.gov/geo/platforms/GPL20nnn/GPL20115/soft/). Then, the probe sequences were aligned with the GENCODE (https://www.gencodegenes.org, version 34) nucleic acid library, and probes that matched successfully were retained. At the same time, we used the average value to represent the expression of genes, and the duplicate probes were removed, leaving the probe with the largest average value. Finally, the expression profile data were divided into two parts: lncRNAs and mRNAs.

2.3. Differential Gene Expression Analysis of lncRNAs and mRNAs. Differential analysis was performed on lncRNAs and mRNAs in NAFLD vs. normal samples using the classic Bayes method provided by the Limma package. |log 2 (fold change)| > log 2 (fold change) cutoff and $P < 0.05$ were considered to be significant.

$$\log 2\,(\mathrm{FC})\mathrm{cutoff} = \overline{|\log 2\,(\mathrm{FC})|} + 1.96 \times \mathrm{SD}$$

$\overline{|\log 2\,(\mathrm{FC})|}$: the mean of|log 2 (FC)|;

SD:standard deviation

Principal component analysis (PCA) was performed by the "FactoMineR package" and the "factoextra package." The differentially expressed (DE) lncRNAs and mRNAs are shown as heat maps and volcano maps by the "pheatmap package" and the "ggplot2 package," respectively.

2.4. Construction of the NLMMN. The miRNA target interactions needed to be identified. The miRcode (http://www.mircode.org/) online tool and Perl were used to predict the potential interactions between DElncRNAs and miRNAs. The "multiMiR package" was used to predict potential interactions between miRNAs and DEmRNAs. The shared miRNAs obtained by these two methods were identified as the predicted DEmiRNAs (pDEmiRNAs). The DElncRNA-miRNA and miRNA−DEmRNA pairs containing pDEmiRNAs were retained. Then, the final DE lncRNA−miRNA−mRNA regulatory relationship in the NLMMN was obtained. The NLMMN was viewed using Cytoscape (http://www.cytoscape.org/; version 3.7.2).

2.5. Gene Ontology (GO) and Kyoto Encyclopedia of Genes and Genomes (KEGG) Enrichment Analyses. The "ClusterProfiler package" was used for GO and KEGG enrichment analyses. GO was used to describe gene functions along three aspects: biological process (BP), cellular component (CC), and molecular function (MF). The significance level was set at a $P < 0.05$ (non or Benjamin Hochberg corrected).

2.6. Inclusion and Exclusion Criteria. The study was conducted in patients who presented to the First Affiliated Hospital of Chongqing Medical University between June 2016 and December 2021. Inclusion criteria were adults with hepatic pathology findings of ≥5% hepatic steatosis. The exclusion criteria were as follows: (a) pregnant women; (b) presence of infection with other viruses (HAV, HBV, HCV, HDV, HEV, and HIV); (c) presence of other liver diseases, such as Wilson's disease; (d) a history of malignancy or hematological diseases; (e) patients who had undergone liver transplantation; (f) suffering from autoimmune diseases; (g) excessive alcohol consumption (>30 g/day in men, >20 g/day in women); (h) taking medication which affects liver status; (i) insufficient laboratory and clinical data. The present study was approved by the Ethics Committee of the First Affiliated Hospital of Chongqing Medical University. Informed consent was obtained from all patients.

2.7. Cell Culture Treatment. HepG2 cells, a human hepatoblastoma cell line, were culture in high glucose Dulbecco's modified Eagle's medium (DMEM) supplemented with 10% fetal bovine serum (FBS) and kept at 37 °C in 5% CO2. Free fatty acids (FFAs) (oleic acid [OA, Sigma-Aldrich, O1383]: palmitic acid [PA, Sigma-Aldrich, P0500], 2:1) were dissolved in a solution of FFA-free bovine serum albumin (FAF-BSA, A8850, Solarbio). To induce fat-overloading of cells, HepG2 cells were exposed to the mixture of FFAs (OA/PA, 2:1) at the final concentration of 1 mM with 1% FAF-BSA 24 h after seeding.

2.8. Oil Red O (ORO) Staining and Determination of Intracellular Lipid Accumulation. HepG2 cells were treated with FFAs for 24 h. According to the manufacturer's instructions, the ORO staining kit (G1262, Solarbio) was used for lipid staining, and the TG detection kit (BC0625, Solarbio) was used to detect intracellular TG content. Each group repeated three individual experiments.

2.9. Cell Transfection. HepG2 cells were seeded into 6-well plates so that the cells were 70% confluent at the time of transfection. To construct LINC00240 over-expression plasmids, human LINC00240 cDNA was synthesized and cloned into a pcDNA3.1 vector by GeneChem (Shanghai, China). An empty plasmid pcDNA3.1 served as the negative control (NC). Transfection was carried out using Lipofectamine 3000 (L3000008, Invitrogen; Thermo Fisher Scientific) according to the manufacturer's instructions. Total RNA was collected 24 h after transfection.

https://doi.org/10.1021/acsomega.2c01801
ACS Omega 2022, 7, 22522−22530

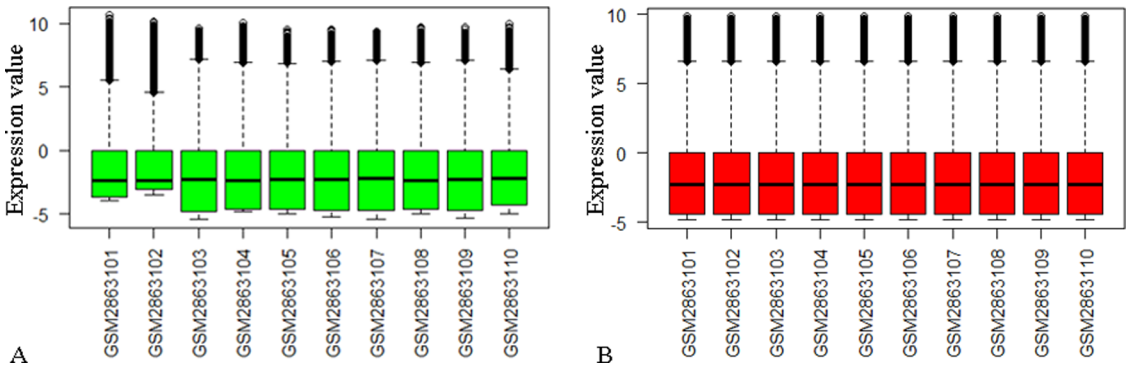

Figure 1. Normalization of the dataset. (A) Before normalization and (B) after normalization.

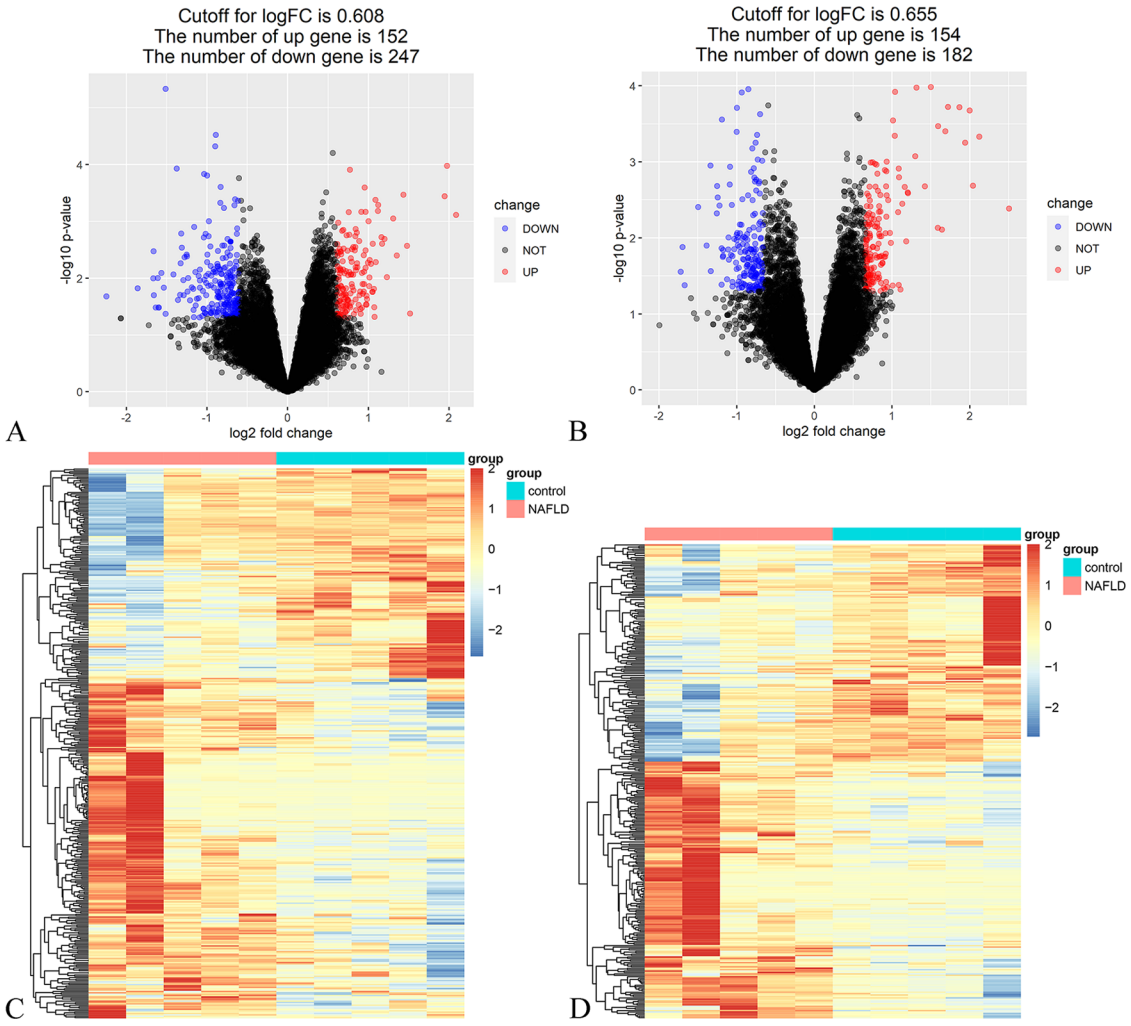

Figure 2. Differential gene expression. (A) Volcano plot of mRNAs, (B) volcano plot of lncRNAs, (C) heatmap of differentially expressed mRNAs, and (D) heatmap of differentially expressed lncRNAs.

2.10. Reactive Oxygen Species (ROS) Assay. Intracellular ROS generation was detected by the ROS detection kit (S0033, Beyotime) according to the manufacturer's instructions. Then, a fluorescence microplate reader was used to measure excitation at 488 nm and emission at 525 nm.

2.11. Real-Time Quantitative Reverse Transcription Polymerase Chain Reaction (qRT−PCR). Total RNA was isolated from patient's liver tissues and HepG2 cells using RNAiso Plus (Takara, Tokyo, Japan). The purified RNA was used as a template to generate first-strand cDNA with a PrimeScript RT reagent Kit with gDNA Eraser (Takara, Tokyo, Japan). The primer sequences used for qRT−PCR are shown in Supporting Table S1.

2.12. Statistical Analysis. The relative RNA expression levels were calculated using the $2^{-\Delta\Delta Ct}$ method. Images were analyzed by Image-Pro Plus 6.0. GraphPad Prism 8 software was used to analyze data with unpaired Student's *t*-test for two groups. The *F* test was used to compare variances, and the unpaired t-test with Welch's correction was used to analyze

https://doi.org/10.1021/acsomega.2c01801
ACS Omega 2022, 7, 22522−22530

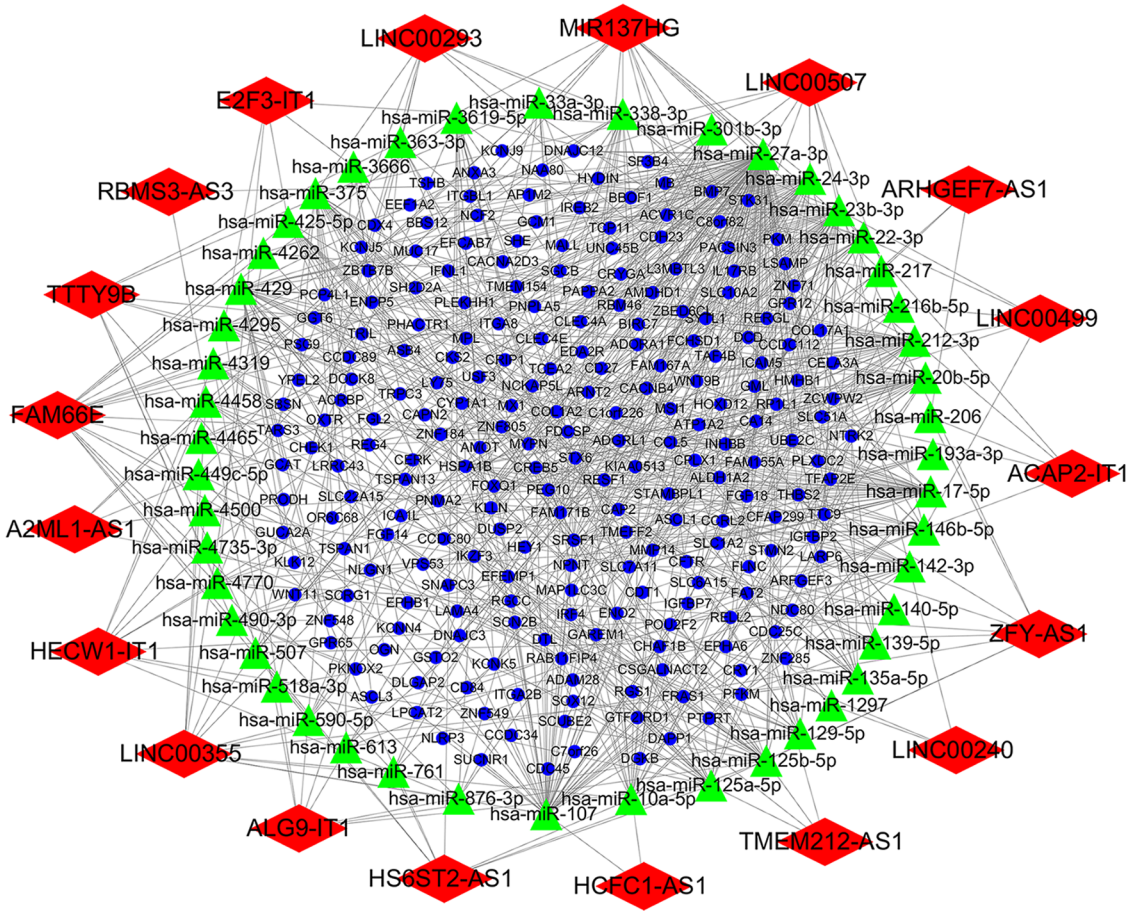

Figure 3. Nonalcoholic fatty liver disease (NAFLD)-related lncRNA−miRNA−mRNA network (NLMMN). Red indicates lncRNAs, blue indicates mRNAs, and green indicates miRNAs.

data when the variances were unequal. $P < 0.05$ was considered statistically significant.

3. RESULTS

3.1. Data Collation. The gene expression data of the GEO database GSE107231, which were generated using the GPL20115 Agilent-067406 Human CBC lncRNA + mRNA microarray V4.0 (probe name version) platform, were downloaded. The sample set of GSE107231 included five NAFLD liver tissues (five males; mean age = 54.8 years) and five normal liver tissues (five males; mean age = 52.8 years). NAFLD was confirmed by pathological examination. We normalized the gene expression data using the Limma package of R software (Figure 1).

3.2. Differential Gene Expression Analysis of lncRNAs and mRNAs. The expression profiles of the data were divided into two parts: lncRNAs and mRNAs, and PCA showed a clear separation between the NAFLD group and the normal group in both parts (Figure S1). A total of 399 differentially expressed mRNAs (DEmRNAs: 152 upregulated and 247 downregulated, |log 2 (fold change)| >0.608 and $P < 0.05$ [NAFLD/normal]) (Table S2) and 336 differentially expressed lncRNAs (DElncRNAs: 154 upregulated and 182 downregulated, |log 2 (fold change)| >0.655 and $P < 0.05$ [NAFLD/normal]) (Table S3) were identified. DERNAs were visualized in volcano and plot heatmaps (Figure 2).

3.3. Construction of the NLMMN. A total of 571 DElncRNA-miRNA interaction pairs were downloaded from miRcode, and 47 372 miRNA−DEmRNA interaction pairs were identified by the "multiMiR packag". After selecting the pairs containing the shared miRNAs, 142 DElncRNA-miRNA interaction pairs (Table S4) and 643 miRNA−DEmRNA (Table S5) interaction pairs were retained to construct the NLMMN (Figure 3). This network contained 19 lncRNAs, 47 miRNAs, and 228 mRNAs.

3.4. GO and KEGG Enrichment Analyses of DEmRNAs. GO and KEGG enrichment analyses were performed on DEmRNAs (Figure 4). The result of GO analysis of all 399 DEmRNAs indicated significant enrichment in six GO terms (Figure 4A and Table 1, $P < 0.05$, Benjamin and Hochberg-corrected), and the result of KEGG analysis showed that two pathways were found to be enriched (Figure 4B: $P < 0.05$). GO analysis results of 228 DEmRNAs in the NLMMN indicated significant enrichment in five GO terms (Figure 4C and Table 2: $P < 0.05$, Benjamin and Hochberg-corrected). Meanwhile, only one pathway (ECM-receptor interaction) was found to be enriched by KEGG enrichment analysis of 228 mRNAs in the NLMMN, which was downregulated. (Figure 4D: $P < 0.05$).

DEmRNAs, differentially expressed mRNAs; GO, Gene Ontology; KEGG, Kyoto Encyclopedia of Genes and Genomes. NLMMN, nonalcoholic fatty liver disease (NAFLD)-related lncRNA−miRNA−mRNA network, ECM, extracellular matrix.

3.5. Information of Patients. A total of three normal liver tissues (one female and two males; age range: 52−57 years;

https://doi.org/10.1021/acsomega.2c01801
ACS Omega 2022, 7, 22522−22530

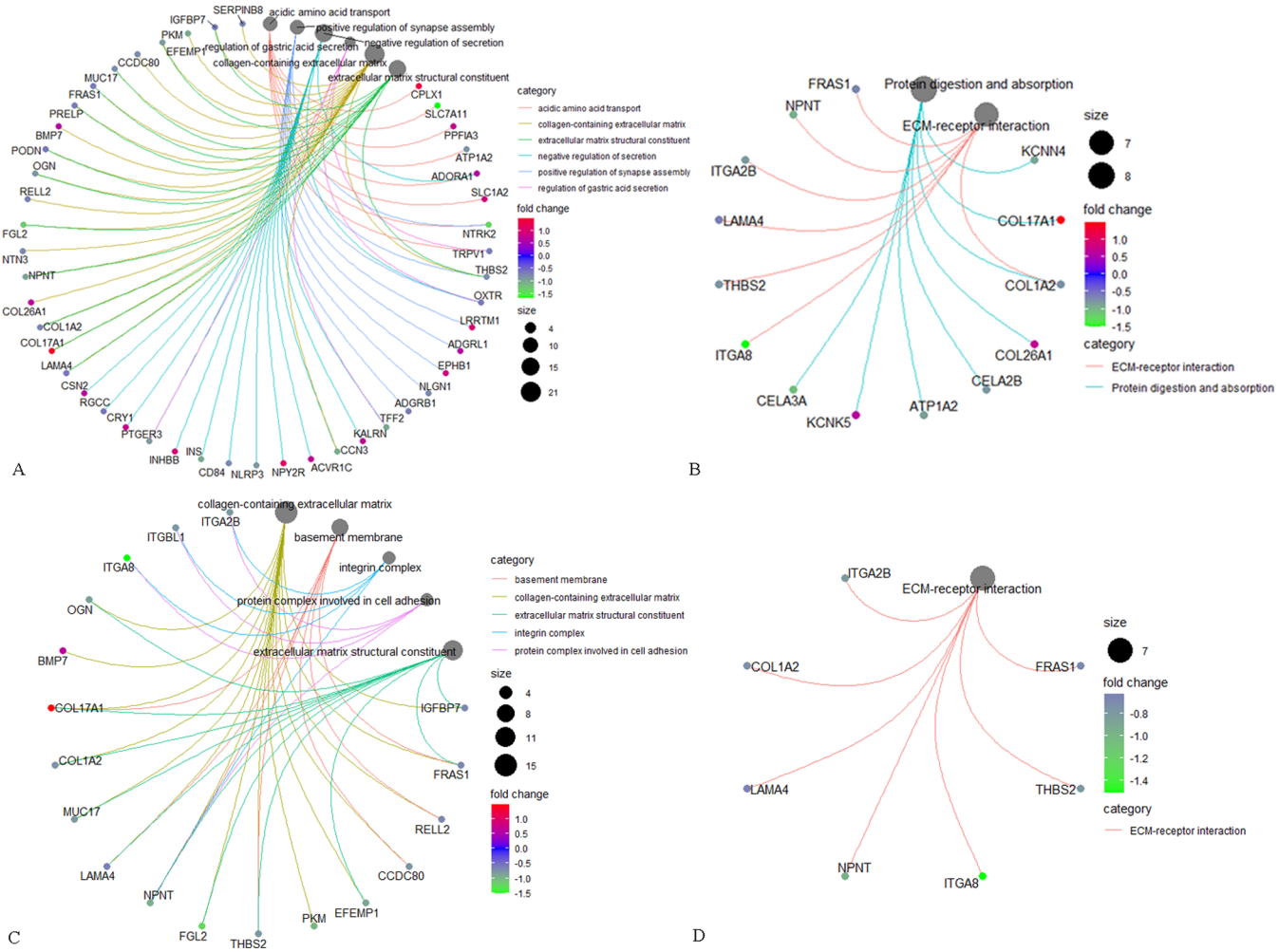

Figure 4. Functional enrichment of DEmRNAs, (A) circle diagram of the DEmRNAs specifically enriched by GO analysis; (B) circle diagram of DEmRNAs specifically enriched by KEGG analysis; (C) circle diagram of the DEmRNAs in the NLMMN specifically enriched by GO analysis; (D) circle diagram of the DEmRNAs in the NLMMN specifically enriched by KEGG analysis. The size of the bubble represents the number of enriched DEmRNAs, and the color represents the *P* value.

Table 1. Enriched GO Terms of the DEmRNAs

terms	pathway description	count	*P*-value	adjusted *P*-value
GO. BP:0015800	acidic amino acid transport	8	2.77×10^{-5}	4.42×10^{-2}
GO. BP:0051965	positive regulation of synapse assembly	8	3.46×10^{-5}	4.42×10^{-2}
GO. BP:0051048	negative regulation of secretion	15	3.77×10^{-5}	4.42×10^{-2}
GO. BP:0060453	regulation of gastric acid secretion	4	4.99×10^{-5}	4.42×10^{-2}
GO.CC:0062023	collagen-containing extracellular matrix	21	2.11×10^{-5}	7.17×10^{-3}
GO.MF:0005201	extracellular matrix structural constituent	13	1.31×10^{-5}	7.02×10^{-3}

Table 2. Enriched GO Terms of the DEmRNAs in the NLMMN

terms	pathway description	count	*P*-value	adjusted *P*-value
GO.CC:0062023	collagen-containing extracellular matrix	15	4.42×10^{-5}	1.21×10^{-2}
GO.CC:0005604	basement membrane	7	8.39×10^{-5}	1.21×10^{-2}
GO.CC:0008305	integrin complex	4	3.49×10^{-4}	3.35×10^{-2}
GO.CC:0098636	protein complex involved in cell adhesion	4	5.02×10^{-4}	3.61×10^{-2}
GO.MF:0005201	extracellular matrix structural constituent	11	3.33×10^{-6}	1.46×10^{-3}

mean age = 55.53 years) and three NAFLD liver tissues (two females and one male; age range: 59−66 years; mean age = 61.7 years) were provided by The First Affiliated Hospital of Chongqing Medical University (Chongqing, China) with pathological sections (Figure 5).

3.6. qRT−PCR of the lncRNAs in the NLMMN in Liver Tissues. qRT−PCR analysis was performed to determine the expression levels of these lncRNAs in the NLMMN. All identified candidate lncRNAs were assayed by qRT−PCR on a sample set of three NAFLD patients and three controls. The

https://doi.org/10.1021/acsomega.2c01801
ACS Omega 2022, 7, 22522−22530

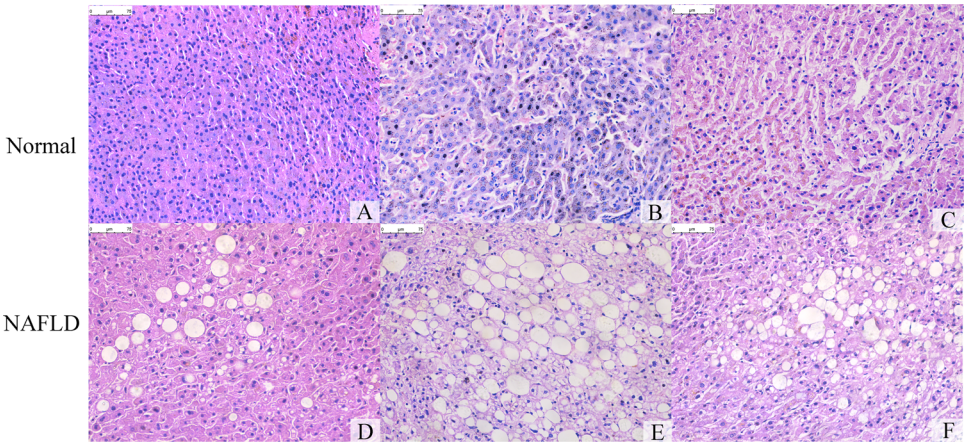

Figure 5. Histopathological examination of liver tissue. (A−C) Normal liver tissues; (D−F) NAFLD liver tissues.

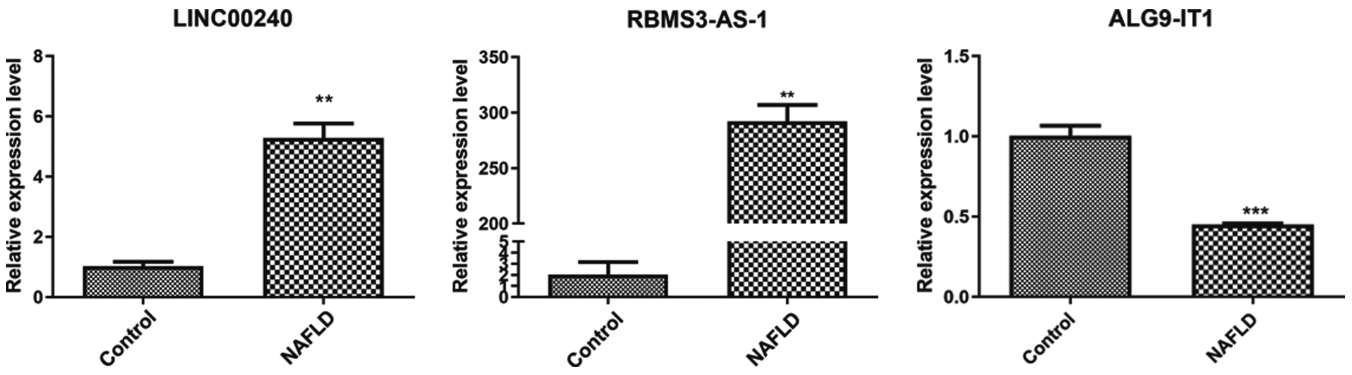

Figure 6. Levels of LINC00240, RBMS3-AS3, and ALG9-IT1 expression in normal liver tissues, and NAFLD liver tissues were detected using qRT−PCR. *P < 0.05, **P < 0.01, ***P < 0.001 by Student's t-test or unpaired t-test with Welch's test.

qRT−PCR results showed that two lncRNAs (LINC00240 and RBMS3-AS3) were upregulated, whereas one (ALG9-IT1) was downregulated in liver tissues of NAFLD patients (Figure 6 and Table S6).

3.7. Upregulation of LINC00240 in HepG2 with Lipid Accumulation. Our previous results suggested that LINC00240 and RBMS3-AS3 were upregulated, whereas one ALG9-IT1 was downregulated in liver tissues of NAFLD patients. After treatment with FFA for 24 h in HepG2, oil red O staining showed that the intracellular lipid droplets increased (Figure 7A), and the intracellular TG content increased significantly at the same time (Figure 7B). These results suggest that the NAFLD cell model was successfully constructed. We redetected these three lncRNAs using qRT-PCR in HepG2 with lipid degeneration by qRT−PCR. The results suggested that LINC00240 was significantly upregulated in HepG2 with lipid accumulation (Figure 7C), while the difference of ALG9-IT1 was not statistically significant (Figure 7D). The expression abundance of RBMS3-AS3 was too low to detect.

3.8. Overexpression of LINC00240 Did Not Affect Lipid Accumulation but Increased ROS Content in HepG2 Cells. In order to explore the role of LINC00240 in NAFLD, we treated HepG2 cells with FFAs to mimic fatty overload conditions. HepG2 cells were transfected with pcDNA3.1 and pcDNA3.1-LINC00240. The results of qRT-PCR showed that transfection of pcDNA3.1-LINC00240 efficiently increased the expression of LINC00240 in HepG2 cells (Figure 7E). Interestingly, overexpression of LINC00240 increased the ROS content in hepG2 (Figure 7F and Table S7). However, overexpression of LINC00240 showed no effect on FFA-induced lipid accumulation in fat-overloading HepG2 cells (Figure 7G and Table S8).

4. DISCUSSION

In recent years, NAFLD has become increasingly prevalent worldwide. However, there is still a lack of effective diagnostic methods and treatment options for NAFLD.[15] As ceRNAs, lncRNAs can participate in the regulation of gene expression. The imbalance of ceRNA and ceRNA networks may have an impact on NAFLD and can also help us understand the disease process and provide new ideas for new therapies.

This study identified key lncRNAs by constructing an NLMMN. Here, we identified 336 DElncRNAs and 399 DEmRNAs based on the GEO database GSE107231. Then, we built an NLMMN, which contains 19 lncRNAs, 47 miRNAs, and 228 mRNAs, and we performed GO and KEGG enrichment analyses. The results of GO enrichment analysis revealed that the mRNAs in the NLMMN were primarily enriched in the extracellular matrix (ECM) (collagen-containing extracellular matrix and extracellular matrix structural constituent). The results of KEGG enrichment analysis showed that the mRNAs in the NLMMN were primarily enriched during ECM-receptor interactions. The occurrence of fibrosis is related to the excessive production of ECM.[16,17] The results of GO and KEGG enrichment analyses suggest that lncRNAs mainly act on the ECM through the ceRNA network. Interestingly, most of these pathways are

https://doi.org/10.1021/acsomega.2c01801
ACS Omega 2022, 7, 22522−22530

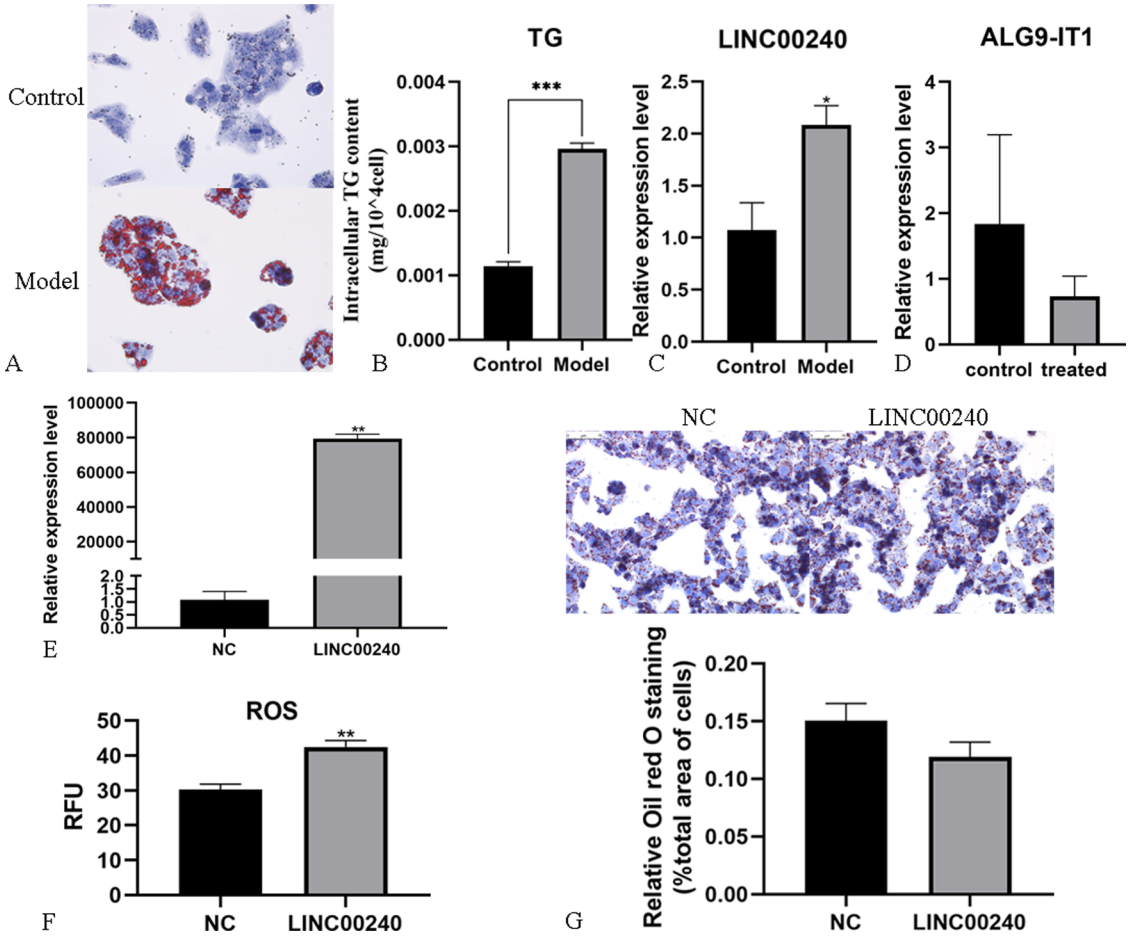

Figure 7. (A) Oil Red O staining of HepG2 cells treated with FFA; (B) intracellular TG content of HepG2 cells treated with FFA; (C) the relative expression level of LINC00240 in FFA-treated and untreated HepG2 cells; (D) the relative expression level of ALG9-IT1 in FFA-treated and -untreated HepG2 cells; (E) detection of the transfection rate of LINC000240 in the overexpression group by qRT−PCR; (F) detection of ROS content in HepG2 cells overexpressing LINC00240; (G) Oil Red O Stain of HepG2 cells overexpressing LINC00240. RFU: relative fluorescence units; Control: FFA-untreated; Model: FFA-treated. Error bars represent the mean ± SEM, $n = 3$,*$P < 0.05$, **$P < 0.01$, ***$P < 0.001$.

downregulated. Excessive accumulation of ECM can lead to fibrosis.[16,17] Therefore, we speculated that lncRNAs may increase the degradation of the ECM through the ceRNA network, thereby reducing the occurrence of liver fibrosis in NAFLD. NAFLD is associated with an increased risk of HCC development, but 20−30% of NAFLD-related HCC cases occur in the absence of cirrhosis.[18] Our study suggested that lncRNAs may play an important role in this phenomenon.

Several studies have revealed that multiple lncRNAs were involved in liver fibrosis, such as metastasis-associated lung adenocarcinoma transcript 1 (MALAT1),[19] transforming growth factor β 2-overlapping transcript 1 (TGFB2-OT1),[20] Alu-mediated p21 transcriptional regulator (APTR),[21] plasmacytoma variant translocation 1 (PVT1),[22] liver fibrosis-associated lncRNA1 (LFAR1),[23] and small nucleolar RNA host gene 7 (SNHG7).[24] And recently, some studies have shown that lncRNAs are involved in inflammation and fibrosis in the progression of liver steatosis. LncRNA nuclear enriched abundant transcript 1 (NEAT1) sponges miR-506 to regulate GLI3 expression to influence inflammation and fibrosis in NAFLD.[25] Zhang et al.[26] found that the expression of lncRNA maternally expressed gene 3 (MEG3) was upregulated in liver tissues of patients with liver fibrosis and cirrhosis caused by NASH. However, the role of lncRNAs in NAFLD fibrosis remains unclear. Our study reveals the importance of lncRNAs in NAFLD fibrosis from a macroscopic perspective for the first time.

In order to further explore the functional lncRNA, we used our patients' liver tissue samples to verify the expression levels of all 19 lncRNAs in the NLMMN by qRT−PCR. The results showed that the expression levels of the two lncRNAs (LINC00240 and RBMS3-AS3) were significantly upregulated, and one lncRNA (ALG9-IT1) was significantly downregulated in the liver tissues from patients with NAFLD compared with the control liver samples. The trend of LINC00240 and ALG9-IT1 expression levels was consistent with the result of bioinformatics analysis, but the result of RBMS3-AS3 was opposite. The results of qRT-PCR showed that the entire expression of RBMS3-AS3 in liver tissue was very low, which may lead to poor stability of the detection data. This may lead to inconsistency between qRT-PCR results and microarray analysis results.

Then we further verified these three DElncRNAs in the HepG2 NAFLD model. The results show that only LINC00240 was significantly upregulated in HepG2 with lipid accumulation. Research by BU et al.[27] showed that LINC00240 could sponge miR-4465 to promote HCC cell proliferation, migration, and invasion. A meta-analysis of 231,355 individuals in a cohort of 82 Europeans revealed that seven single nucleotide polymorphisms (SPNs) were

https://doi.org/10.1021/acsomega.2c01801
ACS Omega 2022, 7, 22522−22530

strongly associated with waist circumference (WC), one of which was located at LINC00240.[28] Increased WC was significantly associated with increased risk of NAFLD,[29] which suggested that LINC00240 might play certain roles in the occurrence and development of NAFLD. However, the biological role of LINC00240 in NAFLD is unclear. We explored the function of LINC00240 in NAFLD in the HepG2 NAFLD model. The increased production of ROS leads to molecular damage called oxidative stress, and NAFLD is influenced by a "multiple parallel-hit model" in which oxidative stress plays a central role.[30] Our results showed that overexpression of LINC00240 did not affect lipid accumulation but increased ROS content in HepG2 cells. This suggested that LINC00240 may have an effect on oxidative stress in hepatocytes. Hepatic stellate cells are key cells for ECM production.[31] And, LX2 is a widely used hepatic stellate cell line.[32] Our current study showed that LINC00240 is involved in apoptosis of LX2 (Wei Xue, Jia Zhang, Wenxiang Huang, unpublished data). This suggested that LINC00240 may be associated with liver fibrosis. And, our team will conduct further research on it.

Although this study successfully constructed an NLMMN, there are some limitations. First, the analyses were based on the microarray dataset GSE107231 downloaded from the GEO database, and the specific stages of NAFLD were not clearly described. In addition, the sample size was small because the liver tissues of NAFLD are very difficult to obtain compared to cancer tissues. Next, we will use laboratory methods to explore the functions of these lncRNAs. It is also hoped that more people will pay attention to the role of lncRNAs in the occurrence and development of NAFLD.

In conclusion, we constructed an NLMMN by analyzing an expression profile of NAFLD from dataset GSE107231 in the GEO database. The results of GO and KEGG enrichment analyses suggest that lncRNAs mainly act on the ECM through the ceRNA network to influence the development of NAFLD. We identified two lncRNAs (LINC00240 and RBMS3-AS3) that were upregulated and one lncRNA (ALG9-IT1) that was downregulated and may be involved in the development of NAFLD by qRT−PCR in patient's liver tissues. But, only LINC00240 was significantly upregulated in HepG2 with lipid accumulation. So, LINC00240, RBMS3-AS3, and ALG9-IT1 might be the novel functional lncRNAs that attenuate liver fibrosis in NAFLD by influencing the ECM through the ceRNA network. Among them, LINC00240 might play a key role. The potential mechanisms of these lncRNAs in NAFLD should be researched to determine their feasibility as diagnostic or therapeutic biomarkers.

■ ASSOCIATED CONTENT

Supporting Information

The Supporting Information is available free of charge at https://pubs.acs.org/doi/10.1021/acsomega.2c01801.

Figure S1. Principal component analysis (PCA) of (a) mRNA and (b) lncRNA expression profiles from the GSE107231 database (PDF)

Table S1. qRT−PCR primers; Table S2. DEmRNAs; Table S3. DElncRNAs; Table S4. DElncRNAs-miRNAs pairs of the ceRNA network; Table S5. DEmRNAs-miRNAs pairs of the ceRNA network; Table S6. The result of qRT-PCR; Table S7. The result of ROS; Table S8. Relative ORO staining (XLSX)

■ AUTHOR INFORMATION

Corresponding Author

Wenxiang Huang − *Department of Geriatrics, The First Affiliated Hospital of Chongqing Medical University, Chongqing 400016, China*; Email: wenxiang_huang@163.com

Authors

Wei Xue − *Chongqing Key Laboratory of Infectious Diseases and Parasitic Diseases, Department of Infectious Diseases, The First Affiliated Hospital of Chongqing Medical University, Chongqing 400016, China*; orcid.org/0000-0001-9780-4934

Jia Zhang − *Chongqing Key Laboratory of Infectious Diseases and Parasitic Diseases, Department of Infectious Diseases, The First Affiliated Hospital of Chongqing Medical University, Chongqing 400016, China*

Yali Zhu − *Chongqing Key Laboratory of Infectious Diseases and Parasitic Diseases, Department of Infectious Diseases, The First Affiliated Hospital of Chongqing Medical University, Chongqing 400016, China*

Complete contact information is available at: https://pubs.acs.org/10.1021/acsomega.2c01801

Author Contributions

Conceptualization, W.X. and W.H.; Data curation, W.X. and J.Z.; Formal analysis, W.X. and J.Z.; Funding acquisition, W.H.; Investigation, J.Z. and Y.Z.; Methodology, W.X. and J.Z.; Project administration, W.H.; Resources, W.H.; Software, W.X.; Supervision, W.H.; Validation, W.X., J.Z., Y.Z., and W.H.; Visualization, W.X.; Writing—original draft, W.X.; Writing—review & editing, W.X., J.Z., Y.Z., and W.H.. All authors will be informed about each step of manuscript processing including submission, revision, revision reminder, etc. via emails from our system or assigned Assistant Editor.

Notes

The authors declare no competing financial interest.

The study was conducted according to the guidelines of the Declaration of Helsinki and approved by the Ethics Committee of the First Affiliated Hospital of Chongqing Medical University, Chongqing, China (protocol code: 2021-371, August 2021).

Publicly available datasets were analyzed in this study. These data can be found here: [(https://www.ncbi.nlm.nih.gov/geo/)/ GSE107231].

■ ACKNOWLEDGMENTS

The authors are deeply grateful to Cheng Yang and Shujun Zhang for their help in this study. The authors appreciate all the staff of the public database and those who share data on the public database. This research was funded by the Chongqing Research Program of Basic Research and Frontier Technology, grant number csct2015jcyjBX0097.

■ REFERENCES

(1) Sayiner, M.; Koenig, A.; Henry, L.; Younossi, Z. M. Epidemiology of Nonalcoholic Fatty Liver Disease and Nonalcoholic Steatohepatitis in the United States and the Rest of the World. *Clin. Liver Dis.* **2016**, *20*, 205−214.

(2) Younossi, Z.; Tacke, F.; Arrese, M.; Chander Sharma, B.; Mostafa, I.; Bugianesi, E.; Wai-Sun Wong, V.; Yilmaz, Y.; George, J.; Fan, J.; Vos, M. B. Global Perspectives on Nonalcoholic Fatty Liver

Disease and Nonalcoholic Steatohepatitis. *Hepatology* **2019**, *69*, 2672−2682.
(3) Tilg, H.; Moschen, A. R. Evolution of inflammation in nonalcoholic fatty liver disease: the multiple parallel hits hypothesis. *Hepatology* **2010**, *52*, 1836−1846.
(4) (a) Bessone, F.; Razori, M. V.; Roma, M. G. Molecular pathways of nonalcoholic fatty liver disease development and progression. *Cell. Mol. Life Sci.* **2019**, *76*, 99−128. (b) Pierantonelli, I.; Svegliati-Baroni, G. Nonalcoholic Fatty Liver Disease: Basic Pathogenetic Mechanisms in the Progression From NAFLD to NASH. *Transplantation* **2019**, *103*, e1−e13. (c) Noureddin, M.; Sanyal, A. J. Pathogenesis of NASH: The Impact of Multiple Pathways. *Curr. Hepatol. Rep.* **2018**, *17*, 350−360.
(5) Younossi, Z. M.; Koenig, A. B.; Abdelatif, D.; Fazel, Y.; Henry, L.; Wymer, M. Global epidemiology of nonalcoholic fatty liver disease-Meta-analytic assessment of prevalence, incidence, and outcomes. *Hepatology* **2016**, *64*, 73−84.
(6) Younossi, Z.; Stepanova, M.; Ong, J. P.; Jacobson, I. M.; Bugianesi, E.; Duseja, A.; Eguchi, Y.; Wong, V. W.; Negro, F.; Yilmaz, H. Y.; et al. Nonalcoholic Steatohepatitis Is the Fastest Growing Cause of Hepatocellular Carcinoma in Liver Transplant Candidates. *Clin. Gastroenterol. Hepatol.* **2019**, *17*, 748.
(7) Younossi, Z.; Anstee, Q. M.; Marietti, M.; Hardy, T.; Henry, L.; Eslam, M.; George, J.; Bugianesi, E. Global burden of NAFLD and NASH: trends, predictions, risk factors and prevention. *Nat. Rev. Gastroenterol. Hepatol.* **2018**, *15*, 11−20.
(8) Cech, T. R.; Steitz, J. A. The noncoding RNA revolution-trashing old rules to forge new ones. *Cell* **2014**, *157*, 77−94.
(9) St Laurent, G.; Wahlestedt, C.; Kapranov, P. The Landscape of long noncoding RNA classification. *Trends Genet.* **2015**, *31*, 239−251.
(10) Kapranov, P.; Cheng, J.; Dike, S.; Nix, D. A.; Duttagupta, R.; Willingham, A. T.; Stadler, P. F.; Hertel, J.; Hackermuller, J.; Hofacker, I. L.; et al. RNA maps reveal new RNA classes and a possible function for pervasive transcription. *Science* **2007**, *316*, 1484−1488.
(11) Kung, J. T. Y.; Colognori, D.; Lee, J. T. Long noncoding RNAs: past, present, and future. *Genetics* **2013**, *193*, 651−669.
(12) (a) Sathishkumar, C.; Prabu, P.; Mohan, V.; Balasubramanyam, M. Linking a role of lncRNAs (long non-coding RNAs) with insulin resistance, accelerated senescence, and inflammation in patients with type 2 diabetes. *Hum. Genomics* **2018**, *12*, No. 41. (b) Ji, E.; Kim, C.; Kim, W.; Lee, E. K. Role of long non-coding RNAs in metabolic control. *Biochim. Biophys. Acta, Gene Regul. Mech.* **2020**, *1863*, No. 194348.
(13) (a) Zhao, X. Y.; Xiong, X.; Liu, T.; Mi, L.; Peng, X.; Rui, C.; Guo, L.; Li, S.; Li, X.; Lin, J. D. Long noncoding RNA licensing of obesity-linked hepatic lipogenesis and NAFLD pathogenesis. *Nat. Commun.* **2018**, *9*, No. 2986. (b) Hanson, A.; Wilhelmsen, D.; DiStefano, J. K. The Role of Long Non-Coding RNAs (lncRNAs) in the Development and Progression of Fibrosis Associated with Nonalcoholic Fatty Liver Disease (NAFLD). *Noncoding RNA* **2018**, *4*, No. 18.
(14) Tay, Y.; Kats, L.; Salmena, L.; Weiss, D.; Tan, S. M.; Ala, U.; Karreth, F.; Poliseno, L.; Provero, P.; Di Cunto, F.; et al. Coding-independent regulation of the tumor suppressor PTEN by competing endogenous mRNAs. *Cell* **2011**, *147*, 344−357.
(15) (a) Wong, V. W.-S.; Adams, L. A.; de Ledinghen, V.; Wong, G. L.; Sookoian, S. Noninvasive biomarkers in NAFLD and NASH - current progress and future promise. *Nat. Rev. Gastroenterol. Hepatol.* **2018**, *15*, 461−478. (b) Friedman, S. L.; Neuschwander-Tetri, B. A.; Rinella, M.; Sanyal, A. J. Mechanisms of NAFLD development and therapeutic strategies. *Nat. Med.* **2018**, *24*, 908−922.
(16) Schwabe, R. F.; Tabas, I.; Pajvani, U. B. Mechanisms of Fibrosis Development in Nonalcoholic Steatohepatitis. *Gastroenterology* **2020**, *158*, 1913−1928.
(17) Khurana, A.; Sayed, N.; Allawadhi, P.; Weiskirchen, R. It's all about the spaces between cells: role of extracellular matrix in liver fibrosis. *Ann. Transl. Med.* **2021**, *9*, No. 728.
(18) Singal, A. G.; El-Serag, H. B. Rational HCC screening approaches for patients with NAFLD. *J. Hepatol.* **2022**, *76*, 195−201.
(19) Yu, F.; Lu, Z.; Cai, J.; Huang, K.; Chen, B.; Li, G.; Dong, P.; Zheng, J. MALAT1 functions as a competing endogenous RNA to mediate Rac1 expression by sequestering miR-101b in liver fibrosis. *Cell Cycle* **2015**, *14*, 3885−3896.
(20) Di Mauro, S.; Scamporrino, A.; Petta, S.; Urbano, F.; Filippello, A.; Ragusa, M.; Di Martino, M. T.; Scionti, F.; Grimaudo, S.; Pipitone, R. M.; et al. Serum coding and non-coding RNAs as biomarkers of NAFLD and fibrosis severity. *Liver Int.* **2019**, *39*, 1742−1754.
(21) Yu, F.; Zheng, J.; Mao, Y.; Dong, P.; Li, G.; Lu, Z.; Guo, C.; Liu, Z.; Fan, X. Long non-coding RNA APTR promotes the activation of hepatic stellate cells and the progression of liver fibrosis. *Biochem. Biophys. Res. Commun.* **2015**, *463*, 679−685.
(22) Zheng, J.; Yu, F.; Dong, P.; Wu, L.; Zhang, Y.; Hu, Y.; Zheng, L. Long non-coding RNA PVT1 activates hepatic stellate cells through competitively binding microRNA-152. *Oncotarget* **2016**, *7*, 62886−62897.
(23) Zhang, K.; Han, X.; Zhang, Z.; Zheng, L.; Hu, Z.; Yao, Q.; Cui, H.; Shu, G.; Si, M.; Li, C.; et al. The liver-enriched lnc-LFAR1 promotes liver fibrosis by activating TGFbeta and Notch pathways. *Nat. Commun.* **2017**, *8*, No. 144.
(24) Xie, Z.; Wu, Y.; Liu, S.; Lai, Y.; Tang, S. LncRNA-SNHG7/miR-29b/DNMT3A axis affects activation, autophagy and proliferation of hepatic stellate cells in liver fibrosis. *Clin. Res. Hepatol. Gastroenterol.* **2021**, *45*, No. 101469.
(25) Jin, S. S.; Lin, X. F.; Zheng, J. Z.; Wang, Q.; Guan, H. Q. lncRNA NEAT1 regulates fibrosis and inflammatory response induced by nonalcoholic fatty liver by regulating miR-506/GLI3. *Eur. Cytokine Network* **2019**, *30*, 98−106.
(26) Zhang, L.; Yang, Z.; Trottier, J.; Barbier, O.; Wang, L. Long noncoding RNA MEG3 induces cholestatic liver injury by interaction with PTBP1 to facilitate shp mRNA decay. *Hepatology* **2017**, *65*, 604−615.
(27) Bu, W. J.; Fang, Z.; Li, W. L.; Wang, X.; Dong, M. J.; Tao, Q. Y.; Zhang, L.; Xu, Y. Q. LINC00240 sponges miR-4465 to promote proliferation, migration, and invasion of hepatocellular carcinoma cells via HGF/c-MET signaling pathway. *Eur. Rev. Med. Pharmacol. Sci.* **2020**, *24*, 10452−10461.
(28) Croteau-Chonka, D. C. Genetic contributions to obesity and related complex traits in the Cebu Longitudinal Health and Nutrition Survey. University of North Carolina at Chapel Hill, 2012, DOI: 10.17615/cw6w-w235.
(29) Ju, D. Y.; Choe, Y. G.; Cho, Y. K.; Shin, D. S.; Yoo, S. H.; Yim, S. H.; Lee, J. Y.; Park, J. H.; Kim, H. J.; Park, D. I.; et al. The influence of waist circumference on insulin resistance and nonalcoholic fatty liver disease in apparently healthy Korean adults. *Clin. Mol. Hepatol.* **2013**, *19*, 140−147.
(30) Mooli, R. G. R.; Mukhi, D.; Ramakrishnan, S. K. Oxidative Stress and Redox Signaling in the Pathophysiology of Liver Diseases. *Compr. Physiol.* **2022**, *12*, 3167−3192.
(31) Tsuchida, T.; Friedman, S. L. Mechanisms of hepatic stellate cell activation. *Nat. Rev. Gastroenterol. Hepatol.* **2017**, *14*, 397−411.
(32) Xu, L.; Hui, A. Y.; Albanis, E.; Arthur, M. J.; O'Byrne, S. M.; Blaner, W. S.; Mukherjee, P.; Friedman, S. L.; Eng, F. J. Human hepatic stellate cell lines, LX-1 and LX-2: new tools for analysis of hepatic fibrosis. *Gut* **2005**, *54*, 142−151.

https://doi.org/10.1021/acsomega.2c01801
ACS Omega 2022, 7, 22522−22530